

# NUMERICAL ANALYSIS OF BONE REMODELLING FOR EQUINE 3<sup>rd</sup> METACARPAL

\*Karol Lewandowski<sup>1,2</sup>, Łukasz Kaczmarczyk<sup>1</sup>, John F. Marshall<sup>2</sup> and Chris J. Pearce<sup>1</sup>

<sup>1</sup>School of Engineering, The University of Glasgow, Glasgow, UK, G12 8LT

<sup>2</sup>School of Veterinary Medicine, The University of Glasgow, Glasgow, UK, G61 1QH

\*k.lewandowski.1@research.gla.ac.uk

## ABSTRACT

The aim of this study was to realistically simulate density growth in the equine 3rd metacarpal bone (MCIII), the most frequently fractured lower limb bone in the Racehorse. A well-established open system thermodynamics approach was adopted into a hierarchical approximation framework. This allowed for an efficient construction of multigrid iterative solvers and solving large problems in 3D including entire bones with their complicated structure. The coupled nonlinear governing equations of mass and linear momentum conservation were implemented in finite element code MOFEM, where tangent stiffness matrix was acquired automatically by using ADOL-C library. Its performance was demonstrated with classical benchmark problems. In order to accurately represent geometry, the final numerical model of the equine bone was generated by processing CT scan images. Furthermore, simplified boundary conditions corresponding to peak forces at mid-stance of a gallop were applied to the bone surface. The obtained density pattern was validated by comparison with the CT scanning data from a cadaver racehorse metacarpal bone. It was shown that the method has the potential to accurately model the effect of loading on bone and could be applied to future studies in order to prevent fatal injuries.

*Key Words: finite element analysis; hierarchical approximation; bone remodelling; racehorse; 3rd metacarpal*

## 1. Introduction

Bones are able to adapt their local density when subjected to mechanical loading. They can change their morphology within days as a result of continuous microstructural tissue turnover and regeneration. Such an adaptation process results in densification of the bone in regions of high loading levels and in resorption of the material in regions of low loading levels. This process is especially essential for racing horses. Due to their intensive training, high tissue accumulation in the distal condyle of metacarpal bones results in the suppression of bone regeneration. This often leads to fatigue fracture, the most commonly reported in the UK during both racing and training [1]. Moving forward, the objective of our study is to develop an efficient diagnostic tool that could help to estimate the risk of fatal injuries by means of finite elements analysis. This paper presents the application of open system thermodynamics approach for functional adaptation in response to external loading. This well-established method was embedded into hierarchical approximation framework of finite element code MOFEM [2]. Derivation of the balance equations was briefly summarised. Application of automatic differentiation with ADOL-C library simplified the derivation of stress tensors and tangent stiffness matrix. Next, a computational solution of a simple one-dimensional problem was presented. It proved that basic functional adaptation assumptions were fulfilled with this approach. Subsequently, three-dimensional model of entire bone was generated, the analysis of which yielded a density pattern at equilibrium state that was then compared with CT scan data from a horse in training for quantitative validation.

## 2. Modelling of density growth

### 2.1. Governing equations

When investigating biological material, density can change in time as opposed to classical mechanics wherein the material density  $\rho$  is conserved within a given body. Following Kuhl and Steinmann [3]

it is assumed that its evolution is driven by the free energy  $\psi_0$  as described by the biological equilibrium equation:

$$\frac{\partial \rho}{\partial t} = R_0, \quad \text{where} \quad R_0 = c \left[ \left[ \frac{\rho_0}{\rho_0^*} \right]^{-m} \psi_0 - \psi_0^* \right] \quad (1)$$

which represents the balance of mass with  $R_0$  - mass source that accounts for density changes. The constant  $c$  characterizes the speed of adaptation,  $n$  and  $m$  are two characteristic exponents,  $\rho_0^*$  is the reference density and  $\psi_0^*$  is the reference free energy, also known as the biological stimulus. To complete the model, an equation of the mass specific free energy density was introduced as the elastic free energy of Neo-Hookean type  $\psi^{neo}$ , weighted by the relative density:

$$\psi_0 = \left[ \frac{\rho_0}{\rho_0^*} \right]^n \psi_0^{neo}, \quad \text{where} \quad \psi_0^{neo} = \frac{\mu}{2} (\text{tr}(\mathbf{C}) - 3) - \mu \ln(J) + \frac{\lambda}{2} \ln J^2, \quad \text{with} \quad J^2 = \det(\mathbf{C}) \quad (2)$$

For porous materials, the exponent  $n$  typically varies between  $1 \leq n \leq 3.5$ . Specifically the MCIII bone exponent  $n$  was based on mechanical testing by Les (1994) [4]. Although bones undergo only small deformations, theory for adaptation was generalised into finite strains. Therefore, free energy was parametrised in terms of right Cauchy-Green deformation tensor  $\mathbf{C} = \mathbf{F}^T \mathbf{F}$ , where  $\mathbf{F}$  is a deformation gradient ( $\mathbf{F} = \nabla \mathbf{u}$ ). Moreover,  $\lambda$  and  $\mu$  are the two Lamé parameters. The free energy equation (2) defines the Piola stress  $\mathbf{P}$  that enters the conservation of momentum equation as:

$$\text{Div}(\mathbf{P}) = 0 \quad (3)$$

With both balance equations at hand, residuals for non-linear solver can be calculated. In this study, tangent stiffness matrix was derived with ADOL-C automatic differentiation - first by deriving 2nd Piola stress tensor  $\mathbf{S}$  from  $\partial \psi / \partial \mathbf{C}$  and then calculating the derivative  $\partial \mathbf{S} / \partial \mathbf{C}$ . Calculations with ADOL-C were in agreement with analytical solutions. As the evolution of the density  $\rho_0^{n+1}$  at time  $t^{n+1}$  is governed by the balance of mass (1), an implicit Euler backward scheme was used for time discretization. Summarised algorithm is shown in the table below.

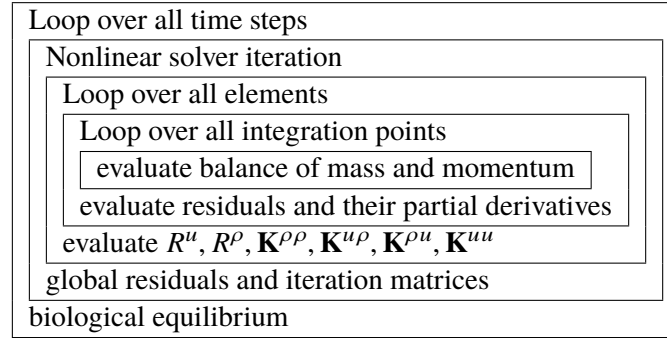


Table 1: Computational algorithm for monolithic solution approach.

## 2.2. Benchmark problem

To depict the features of open system thermodynamics approach, a simple homogeneous bar of unit size is presented here. The following parameters were used: elasticity modulus  $E = 1$ , Poisson's ratio of  $\nu = 0$ . The reference density was chosen to be  $\rho_0^* = 1$  and energy stimulus was  $\psi_0^* = 1$ . To ensure uniqueness and stability of the solution, exponents of growth were  $m = 3$  and  $n = 2$ . Time integration was performed with time steps of  $\Delta t = 0.1$ . The specimen was axially loaded by multiple step loading function as illustrated in Figure 1 below. The corresponding deformation proves the non-linearity of the problem. The time dependent nature of the balance of mass was visualised. Curves of primary unknowns demonstrated the relaxation towards biological equilibrium, the state when density converged to a final value for particular loading magnitude.

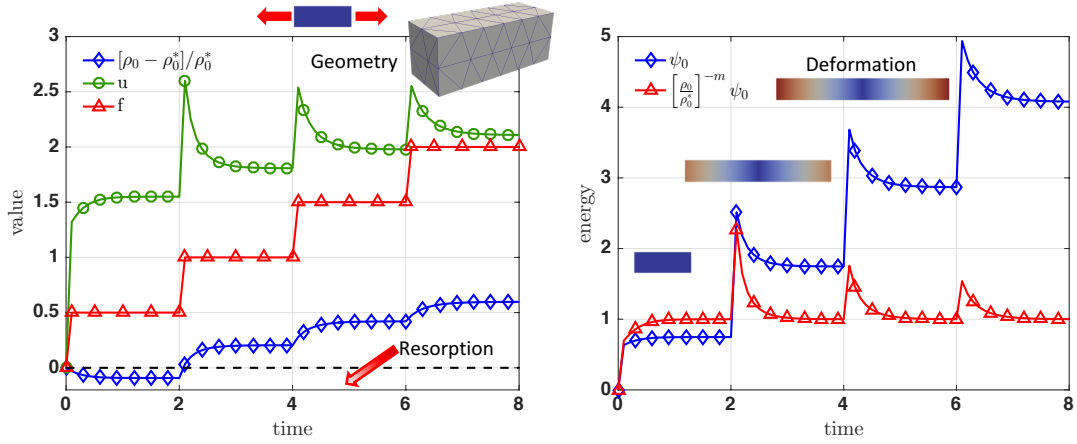


Figure 1: One-dimensional model problem. Evolution of density  $\rho_0$ , displacements  $u$  and energy values  $\psi$  and relative energy  $[\rho_0/\rho_0^*]^{-m} \psi$ .

### 3. Numerical example

Proposed density growth model was subsequently applied to a subject-specific three-dimensional, full-scale model of equine MCIII bone derived from CT scanning. Initial density distribution was homogeneous in this study. However, developed code has a capability of mapping density data into finite element mesh. Segmented geometry was discretised into 7255 high quality (shape ratio  $> 0.3$ ) quadratic tetrahedrons. 2<sup>nd</sup> order geometry elements were used for high-detail representation as shown in Figure 2. Boundary conditions have been simplified to two representative forces (5 kN each) spanning over a small area based on pressure film studies by Brama (2001) [5]. They are often considered as an equivalent of peak force at the mid-stance of a horse gait. Furthermore, degrees of freedom at the proximal end were fixed. In reality, metacarpal bone articulates with proximal phalanx bone, which will be the subject of future contact mechanics studies. The analysis was divided into 100 time steps with the constant time step size of  $\Delta t = 0.5$  [d]. External forces were applied by linearly increasing their magnitude within first 5 time steps and held constant thereafter. Material and model parameters (Table 2) were adopted based on previous studies of human bones [6]. Higher stiffness of equine bones derived from mechanical testing studies [4] was also taken into account. Results of the analysis are presented in Figure 2b where density

Parameter	Description	Value
$E$	Young's modulus	9000 [MPa] Les (1994) [4]
$\nu$	Poisson ratio	0.3 [-]
$\rho_0^*$	Initial density	1.0 [g/cm <sup>3</sup> ]
$\psi_0^*$	Target energy	0.0275 [MPa] Waffenschmidt (2012) [6]
$c$	Density growth velocity	5.0 [d/cm <sup>2</sup> ]
$m$	Algorithmic exponent	3.35 [-]
$n$	Porosity exponent	2.35 [-] Les (1994) [4]

Table 2: Material parameters used for the simulations.

maps at four different points in time (0, 10, 20, 30) [d] are visualised. Great densification occurred just after reaching maximum level of the loading, particularly in the proximity of applied forces, where the high levels of strain energy were expected. In the areas not affected by the loading, material degradation can be observed. After time 30 density levels on entire bone became saturated, biological equilibrium was achieved, hence no changes appeared thereafter. At this point, density was measured in the region of the sagittal grooves as demonstrated in Figure 2c, the most frequent site of a fracture initiation in MCIII bone. Simultaneously, the density of bone in the same region of a horse in training was derived from the CT scan using quantitative computed tomography with appropriate (dipotassium phosphate) phantoms.

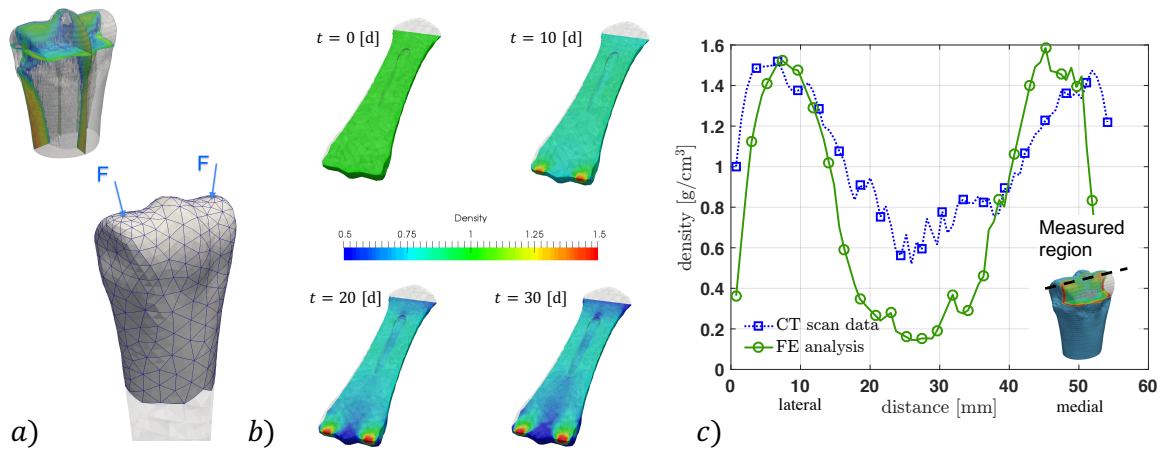


Figure 2: a) Geometry of the distal end of the MCIII bone and finite element mesh with applied concentrated forces. b) Density evolution in the proximal tibia at four different points in time. c) Variation of bone mineral density in the region of interest derived from FEM and CT.

Subsequently, both resultant data were compared and found to be in satisfying agreement.

#### 4. Conclusions

Despite certain limitations of this study, it showed that a reasonable agreement with experimental data can be achieved. Using the theory of open systems thermodynamics allowed to simulate natural behaviour of hard biological tissues. It is believed that results can be greatly refined by improving many aspects of this approach, like more accurate boundary conditions and taking anisotropy of density growth into account. The proposed computational method may have a great potential to identify the risk of fracture related to changes in bone mineral density.

#### Acknowledgements

The authors are particularly grateful to the staff of the Small Animal Hospital, where the CT scans of the equine metacarpal bone were performed. Lord Kelvin Adam Smith PhD Scholarship is acknowledged for providing financial support.

#### References

- [1] T D H Parkin, P D Clegg, N P French, C J Proudman, C M Riggs, E R Singer, P M Webbon, and K L Morgan. Risk factors for fatal lateral condylar fracture of the third metacarpus/metatarsus in UK racing. *Equine veterinary journal*, 37(3):192–199, 2005.
- [2] MoFEM: Mesh Oriented Finite Element Method code. <http://mofem.eng.gla.ac.uk/>.
- [3] E. Kuhl and P. Steinmann. Theory and numerics of geometrically non-linear open system mechanics. *International Journal for Numerical Methods in Engineering*, 58(11):1593–1615, 2003.
- [4] C. M. Les, Joyce H. Keyak, S. M. Stover, K. T. Taylor, and A. J. Kaneps. Estimation of material properties in the equine metacarpus with use of quantitative computed tomography. *Journal of Orthopaedic Research*, 12(6):822–833, 1994.
- [5] P Brama, D Karssenbergh, Barneveld, and P R van Weeren. Contact areas and pressure distribution on the proximal articular surface of the proximal phalanx under sagittal plane loading. *Equine veterinary journal*, 33(1):26–32, 2001.
- [6] T. Waffenschmidt, A. Menzel, and E. Kuhl. Anisotropic density growth of bone - A computational micro-sphere approach. *International Journal of Solids and Structures*, 49(14):1928–1946, 2012.